The University of Adelaide

School of Chemical Engineering

Cooperative Research Centre for Clean Power from Lignite

Physical Modelling of Mixing Between Rectangular Jets Present in Tangentially Fired Brown Coal Boilers

Ph.D. Thesis

Alessio Angelo Scarsella

Appendix C

C. Transverse Flow Visualization

Sub-sections C.1 and C.2 present sequential instantaneous images of the transverse experiments of the primary jets at axial stations of x/D =0.1, 1, 2, 4, 6, and 8, velocity ratios of λ=0, 0.55, 1.4, 2.8 and 3.6 and Secondary jets at axial stations of x/D =0.5, 1, 2, 4, 6 and 8 and velocity ratios of λ =0.55, 1.4, 2.8, 3.6 and ∞.

C.1. Transverse Flow Visualization of the Primary Jet.

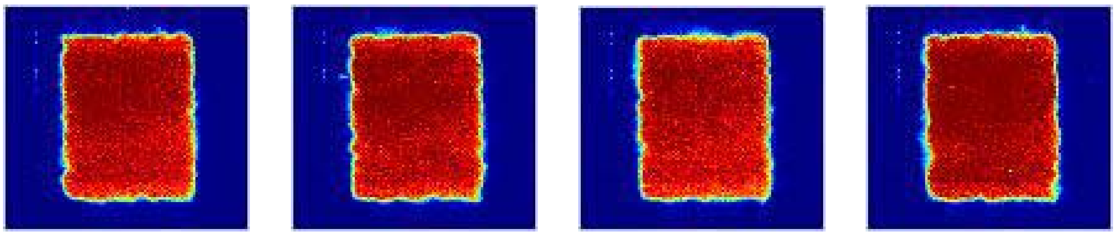

t =0 | t =0.05s | t =0.1s | t =0.15s

Figure C. 1: Instantaneous flow visualisation of the normalised concentration for the primary jet at x/D=0.1, at 0.05 second intervals and λ = 0, γ=0, κ =0.

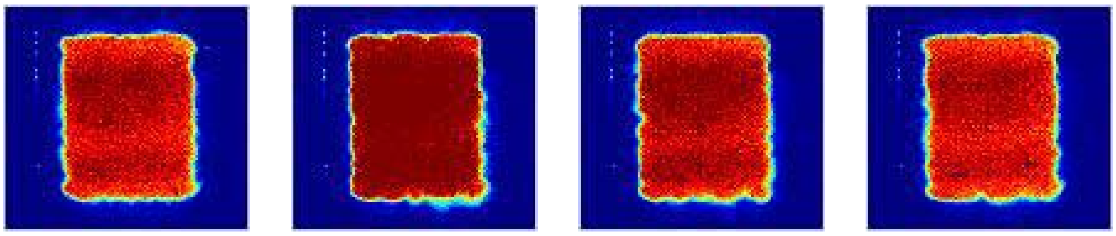

t =0 | t =0.05s | t =0.1s | t =0.15s

Figure C. 2: Instantaneous flow visualisation of the normalised concentration for the primary jet at x/D=0.1, at 0.05 second intervals and λ = 0.55, γ=0.3, κ =0.18.

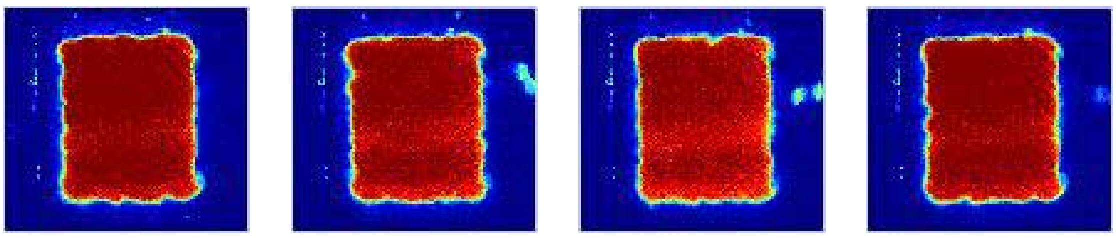

t =0 | t =0.05s | t =0.1s | t =0.15s

Figure C. 3: Instantaneous flow visualisation of the normalised concentration for the primary jet at x/D=0.1, at 0.05 second intervals and λ = 1.4, γ=1.96, κ =1.18.

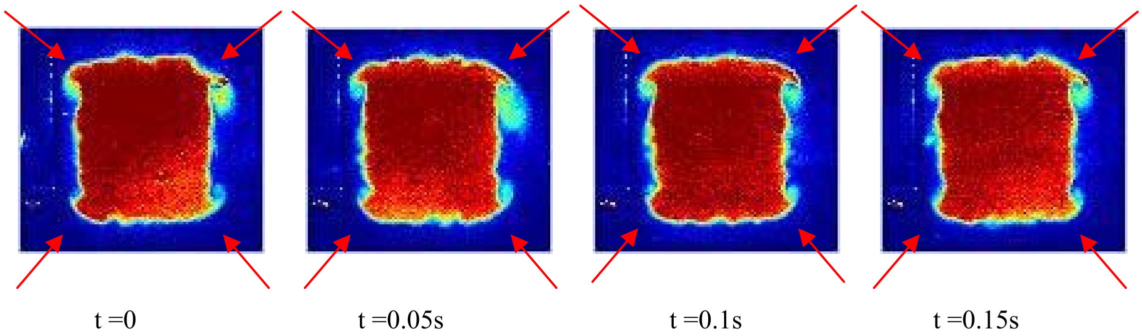

Figure C. 4: Instantaneous flow visualisation of the normalised concentration for the primary jet at *x/D*=0.1, at 0.05 second intervals and λ = 2.8, γ=7.84, κ =4.7. Red arrows illustrate the distortion of the primary jet fluid with a change in velocity gradient due to the higher velocity ratio.

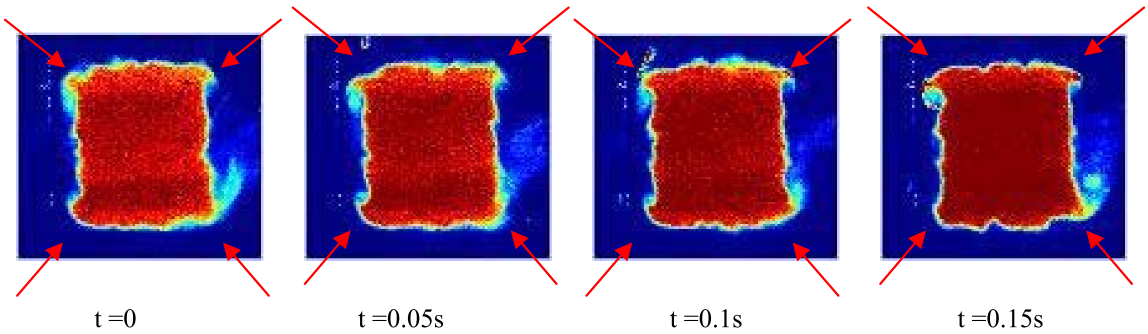

Figure C. 5: Instantaneous flow visualisation of the normalised concentration for the primary jet at *x/D*=0.1, at 0.05 second intervals and λ = 3.6, γ=12.96, κ =7.78. Red arrows illustrate the distortion of the primary jet fluid with a change in velocity gradient due to the higher velocity ratio.

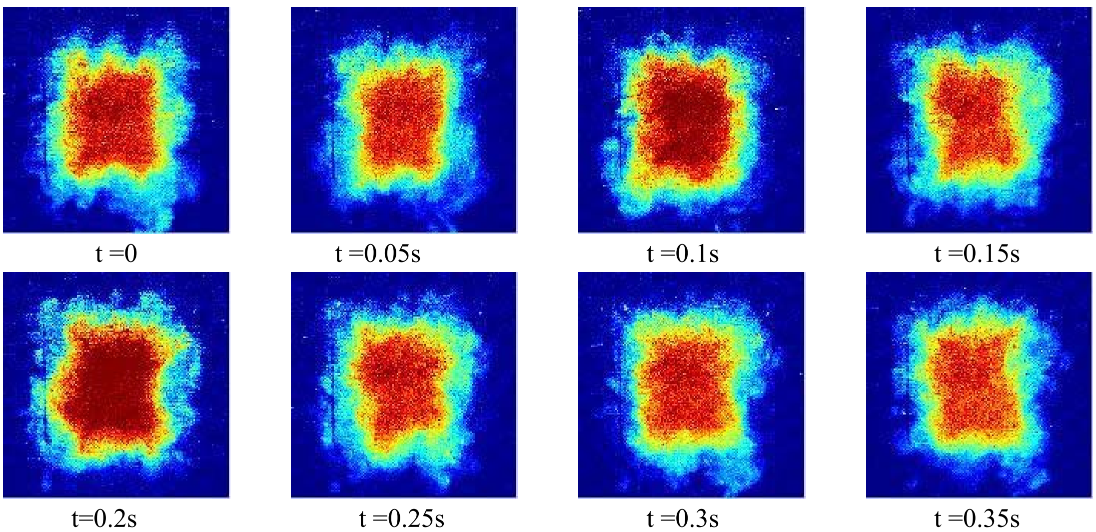

Figure C. 6: Instantaneous flow visualisation of the normalised concentration for the primary jet at *x/D*=1, at 0.05 second intervals and λ = 0, γ=0, κ =0. Red arrows indicate oscillation of the lobes of the primary structure.

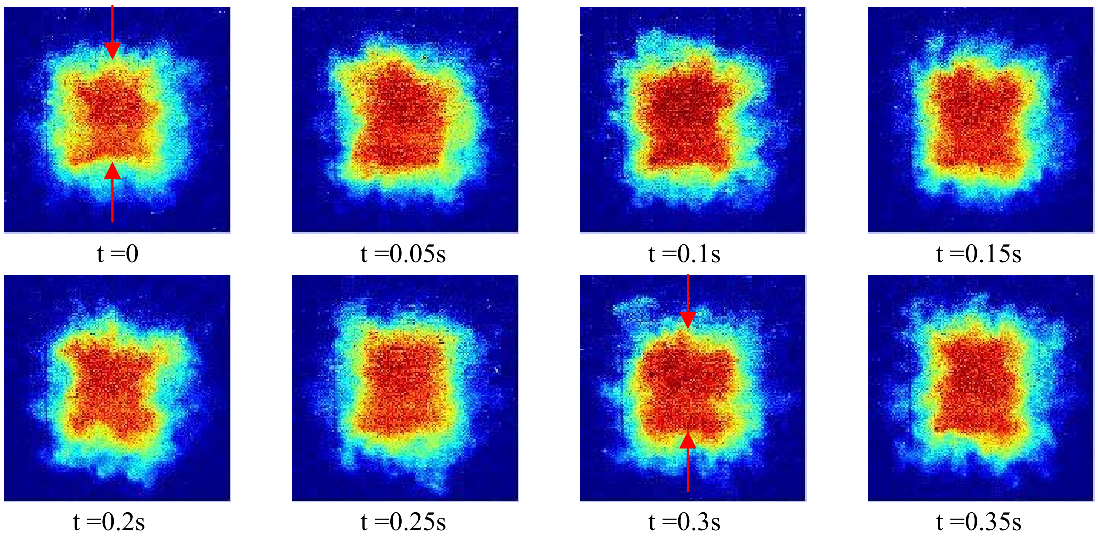

Figure C. 7: Instantaneous flow visualisation of the normalised concentration for the primary jet at *x/D*=1, at 0.05 second intervals and λ = 0.55, γ=0.3, κ =0.18. Red arrows indicate out of phase shortening of the primary structure in the *y*-direction.

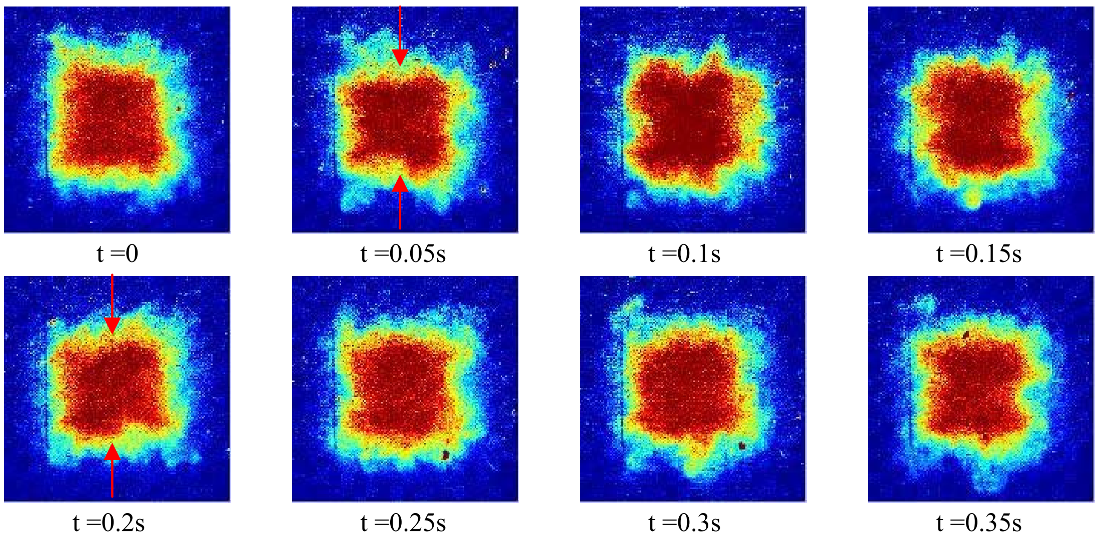

Figure C. 8: Instantaneous flow visualisation of the normalised concentration for the primary jet at *x/D*=1, at 0.05 second intervals and λ = 1.4, γ=1.96, κ =1.18. Red arrows indicate out of phase shortening of the primary structure in the *y*-direction.

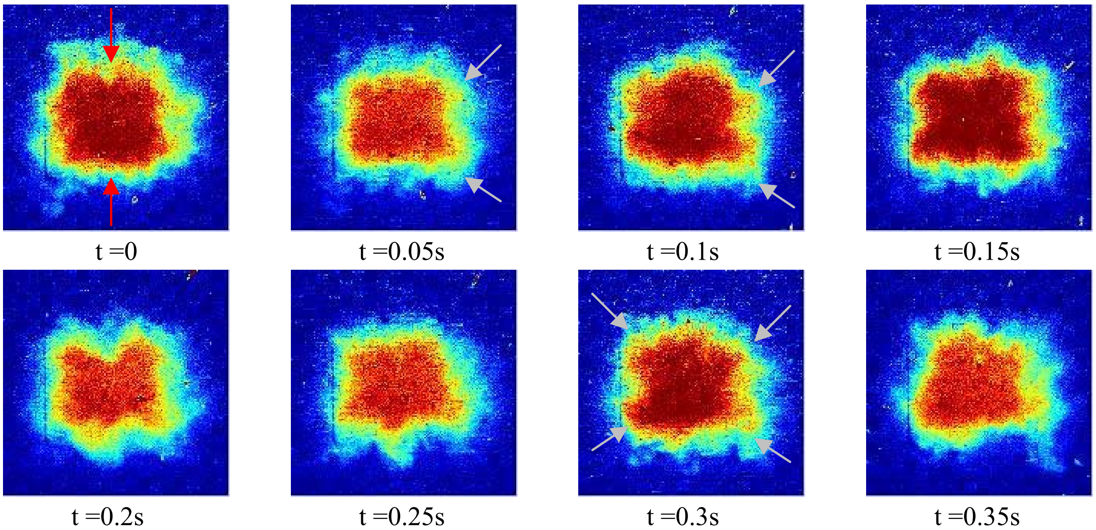

Figure C. 9: Instantaneous flow visualisation of the normalised concentration for the primary jet at x/D=1, at 0.05 second intervals and λ = 2.8, γ=7.84, κ =4.7. Red arrows indicate the out of phase shortening of the primary structure in the y-direction, and the white arrows illustrate primary jet distortion proximity to the corners due to the change in velocity gradient at higher velocity ratios.

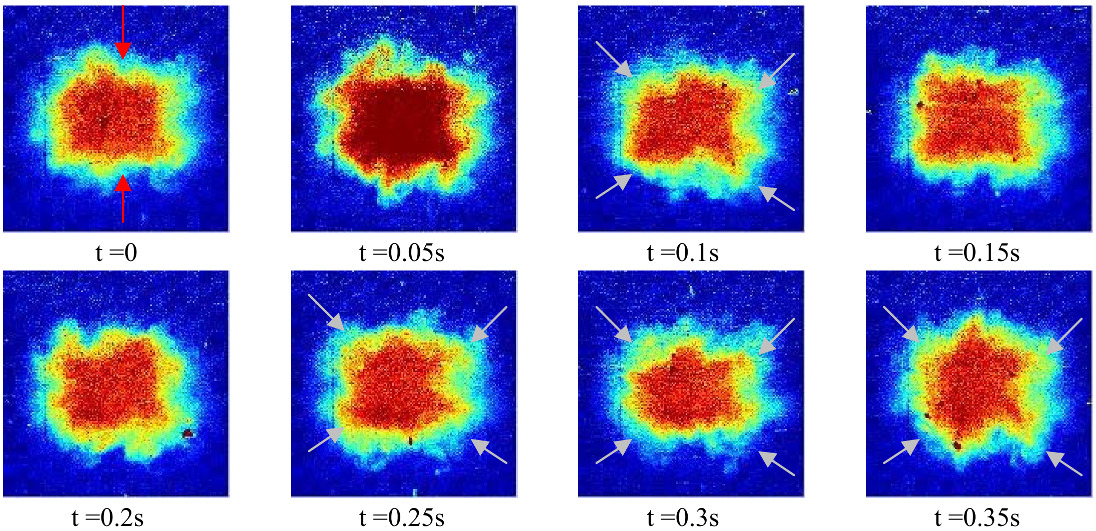

Figure C. 10: Instantaneous flow visualisation of the normalised concentration for the primary jet at x/D=1, at 0.05 second intervals and λ = 3.6 γ=12.96, κ =7.78. Red arrows indicate the out of phase shortening of the primary structure in the y-direction, and the white arrows illustrate primary jet distortion proximity to the corners due to the change in velocity gradient at higher velocity ratios.

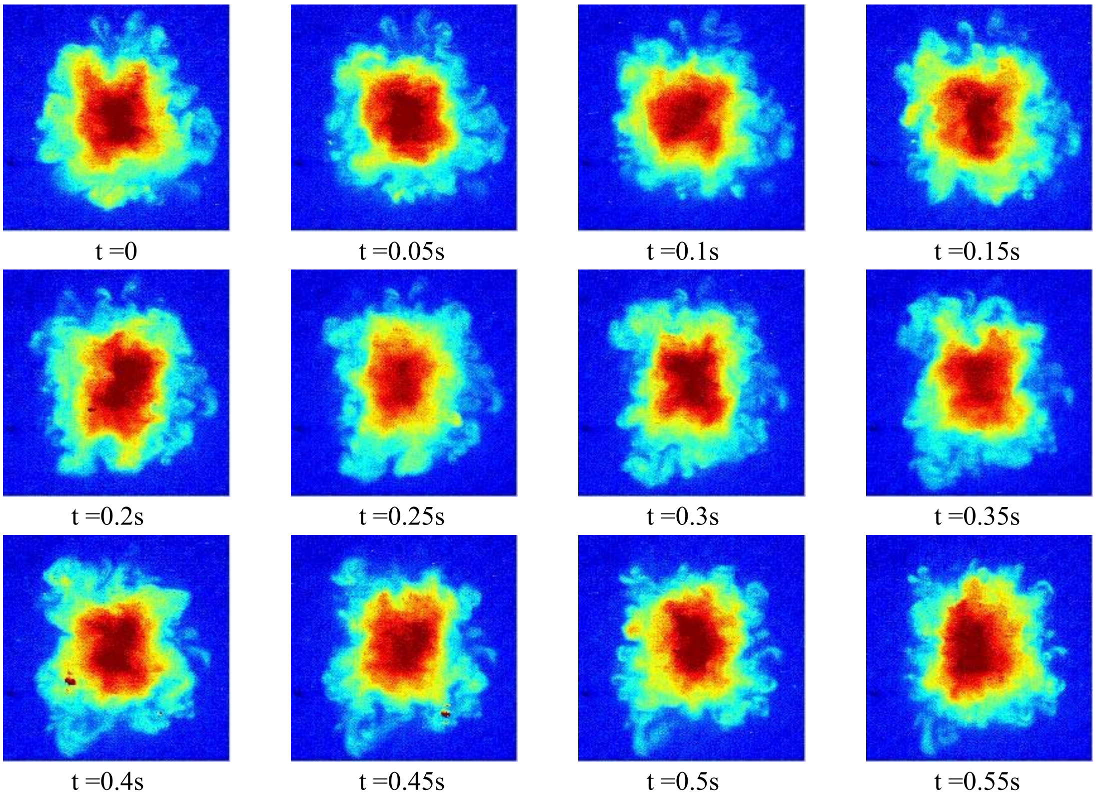

Figure C. 11: Instantaneous flow visualisation of the normalised concentration for the primary jet at *x/D*=2, at 0.05 second intervals and $\lambda = 0$, γ=0, κ =0.

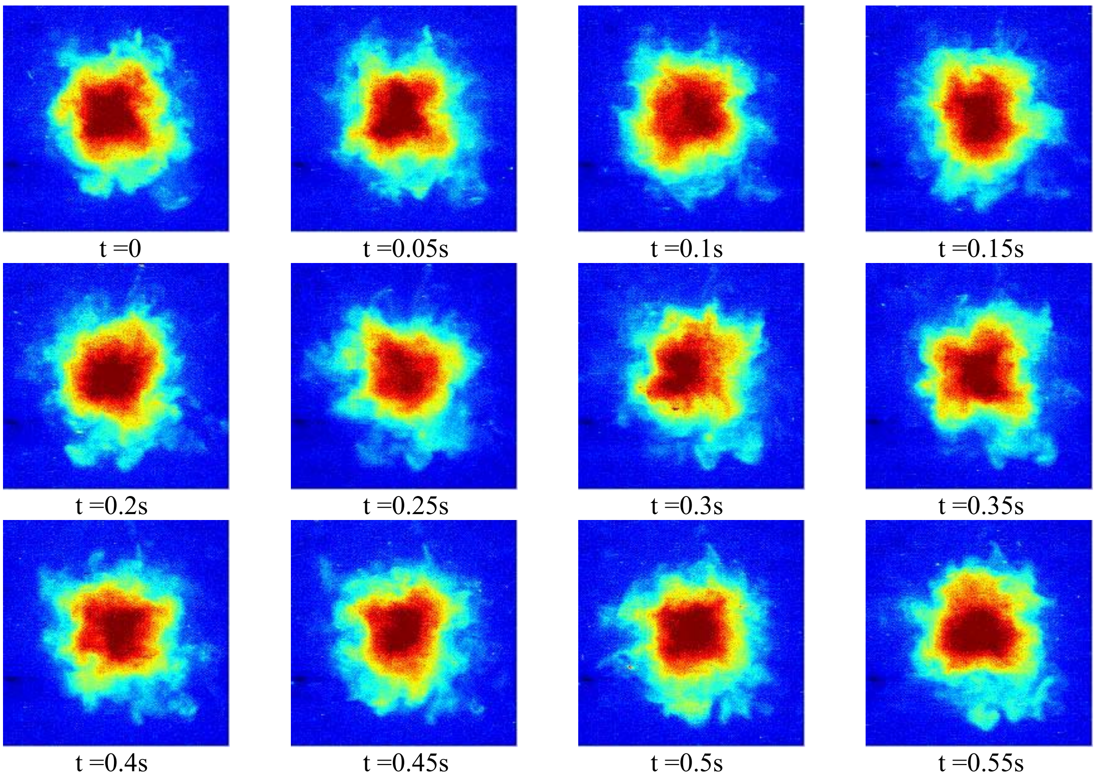

Figure C. 12: Instantaneous flow visualisation of the normalised concentration for the primary jet at *x/D*=2, at 0.05 second intervals and $\lambda = 0.55$, γ=0.3, κ =0.18.

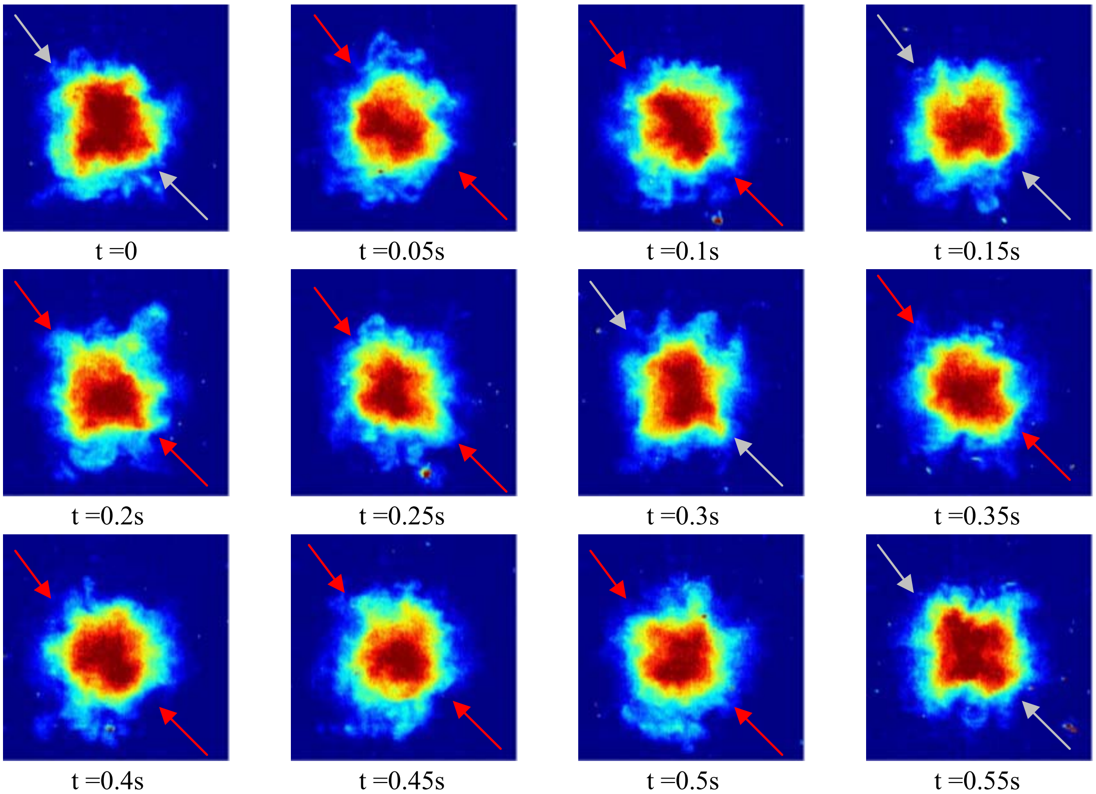

Figure C. 13: Instantaneous flow visualisation of the normalised concentration for the primary jet at *x/D*=2, at 0.05 second intervals and λ = 1.4, γ=1.96, κ =1.18. The red arrows highlight the out of phase distortion of the primary jet whilst the white arrows indicate the original rectangular shape.

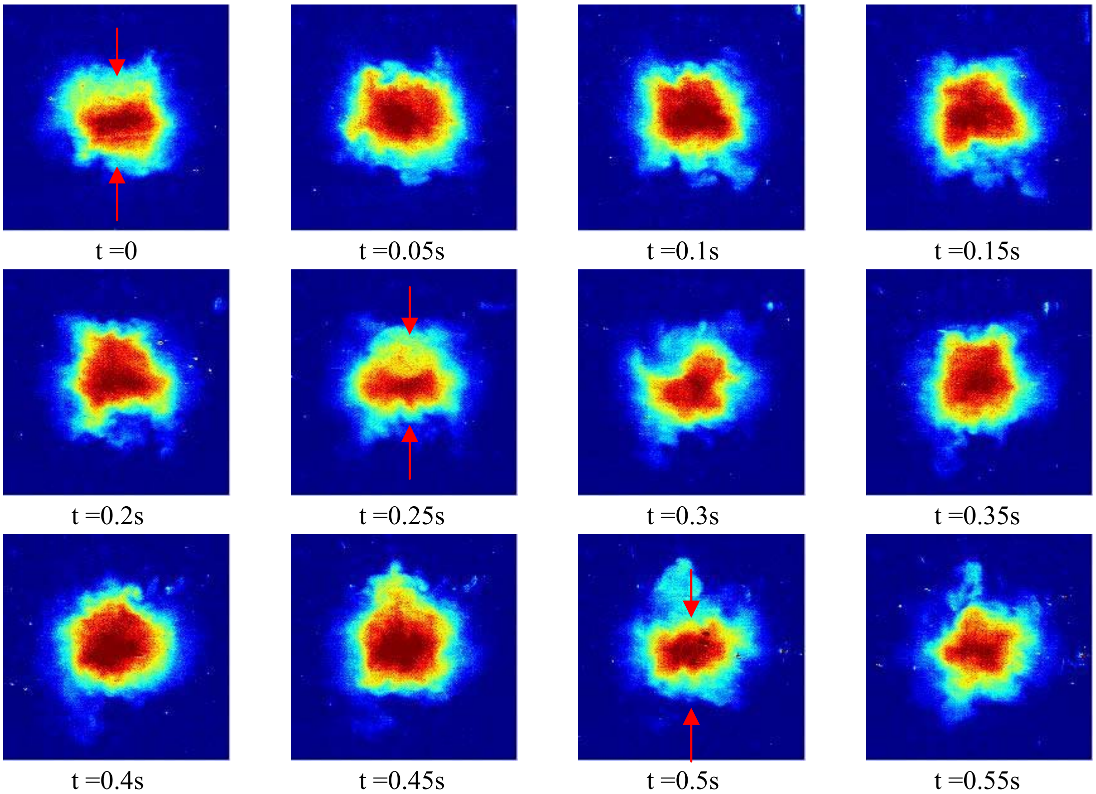

Figure C. 14: Instantaneous flow visualisation of the normalised concentration for the primary jet at *x/D*=2, at 0.05 second intervals and λ = 2.8, γ=7.84, κ =4.7. The red arrows highlight the out of phase shortening in the *y*-direction of the jet.

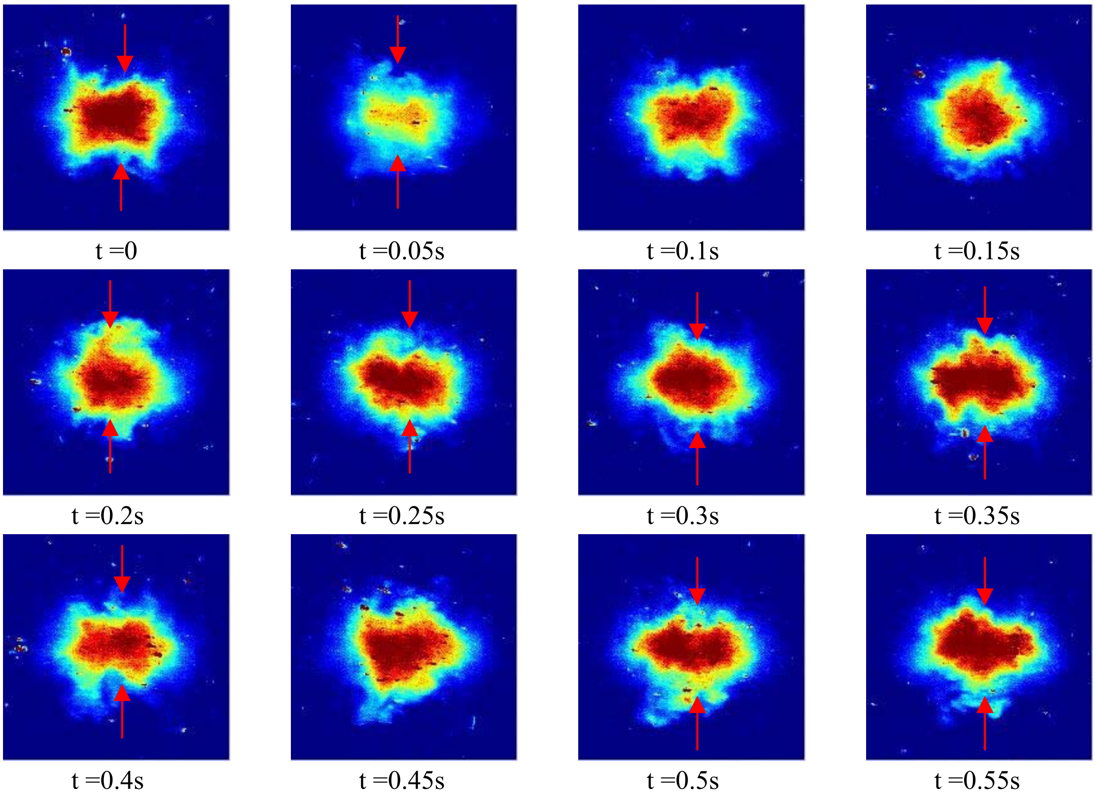

Figure C. 15: Instantaneous flow visualisation of the normalised concentration for the primary jet at *x/D*=2, at 0.05 second intervals and λ = 3.6 γ =12.96, κ =7.78. The red arrows highlight the out of phase shortening in the *y*-direction of the jet.

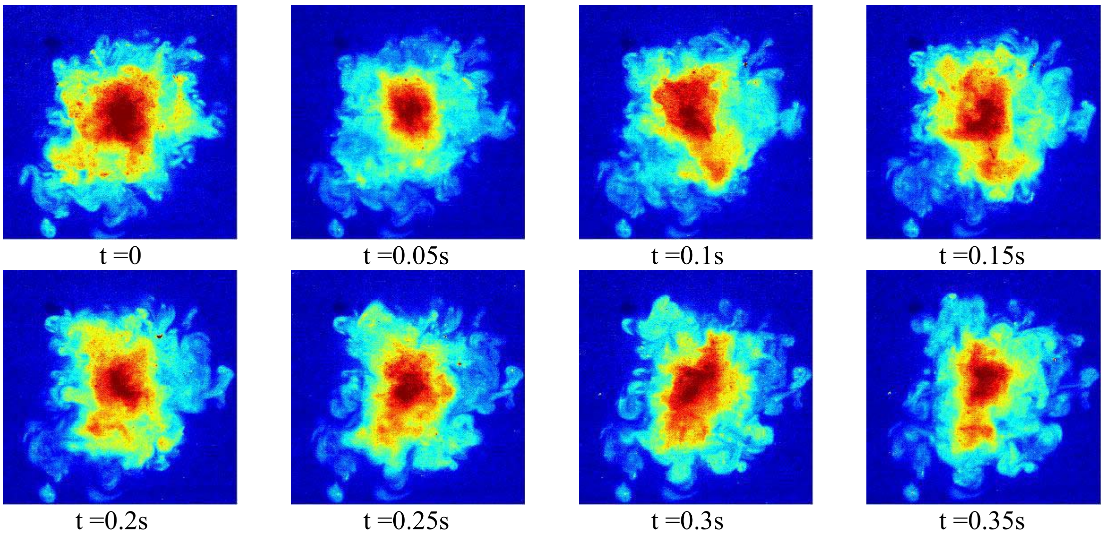

Figure C. 16: Instantaneous flow visualisation of the normalised concentration for the primary jet at *x/D*=4, at 0.05 second intervals and λ = 0, γ=0, κ =0.

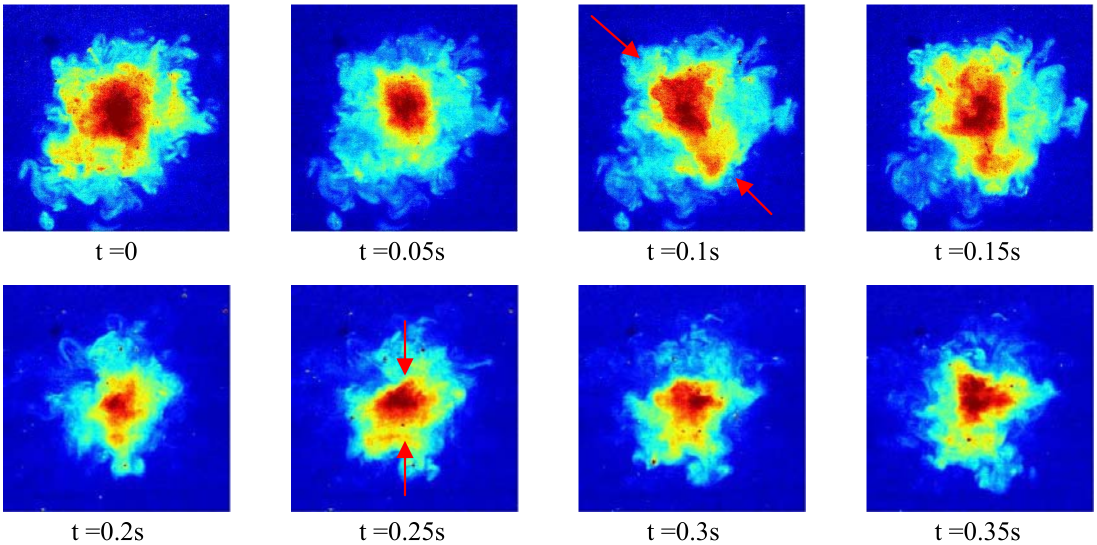

Figure C. 17: Instantaneous flow visualisation of the normalised concentration for the primary jet at x/D=4, at 0.05 second intervals and λ = 0.55, γ=0.3, κ =0.18. The red arrows indicate the out of phase distortion of the primary jet.

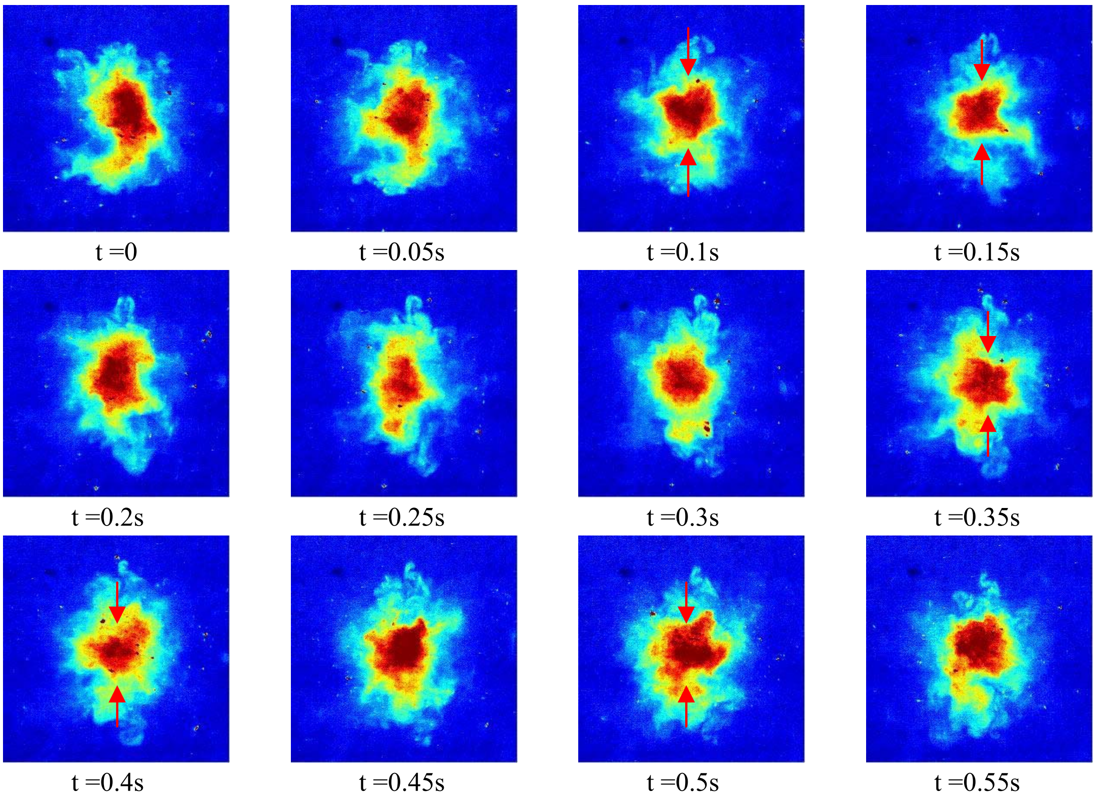

Figure C. 18: Instantaneous flow visualisation of the normalised concentration for the primary jet at x/D=4, at 0.05 second intervals and λ = 1.4, γ=1.96, κ =1.18. The red arrows indicate the out of phase shortening of the jet in the y-direction.

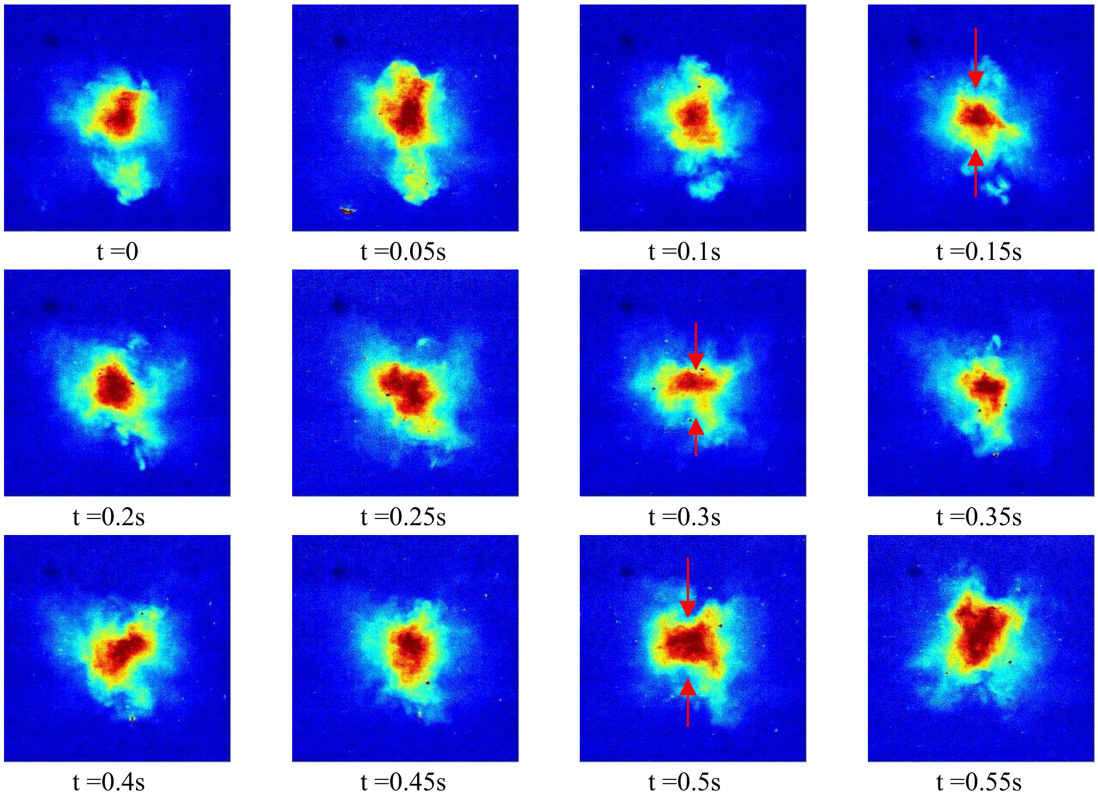

Figure C. 19: Instantaneous flow visualisation of the normalised concentration for the primary jet at *x/D*=4, at 0.05 second intervals and λ = 2.8, γ=7.84, κ =4.7. The red arrows indicate the out of phase shortening of the jet in the *y*-direction.

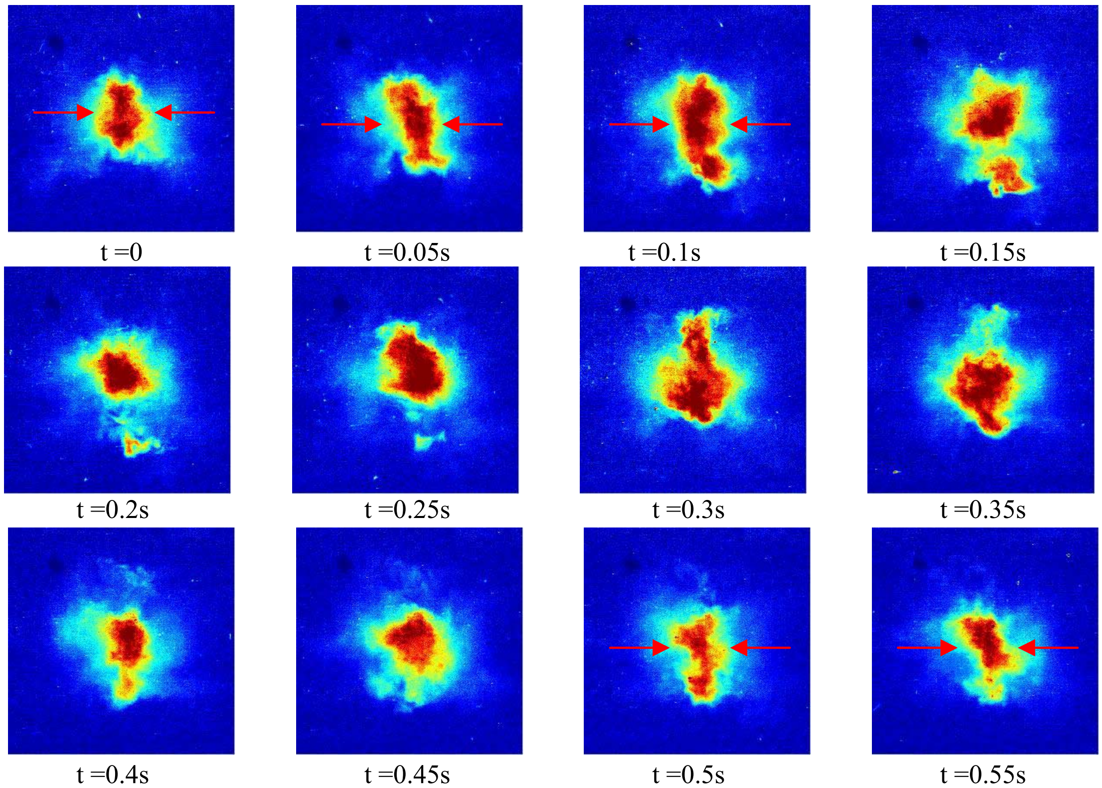

Figure C. 20: Instantaneous flow visualisation of the normalised concentration for the primary jet at *x/D*=4, at 0.05 second intervals and λ = 3.6, γ=12.96, κ =7.78. The red arrows indicate the out of phase shortening of the jet in the *z*-direction.

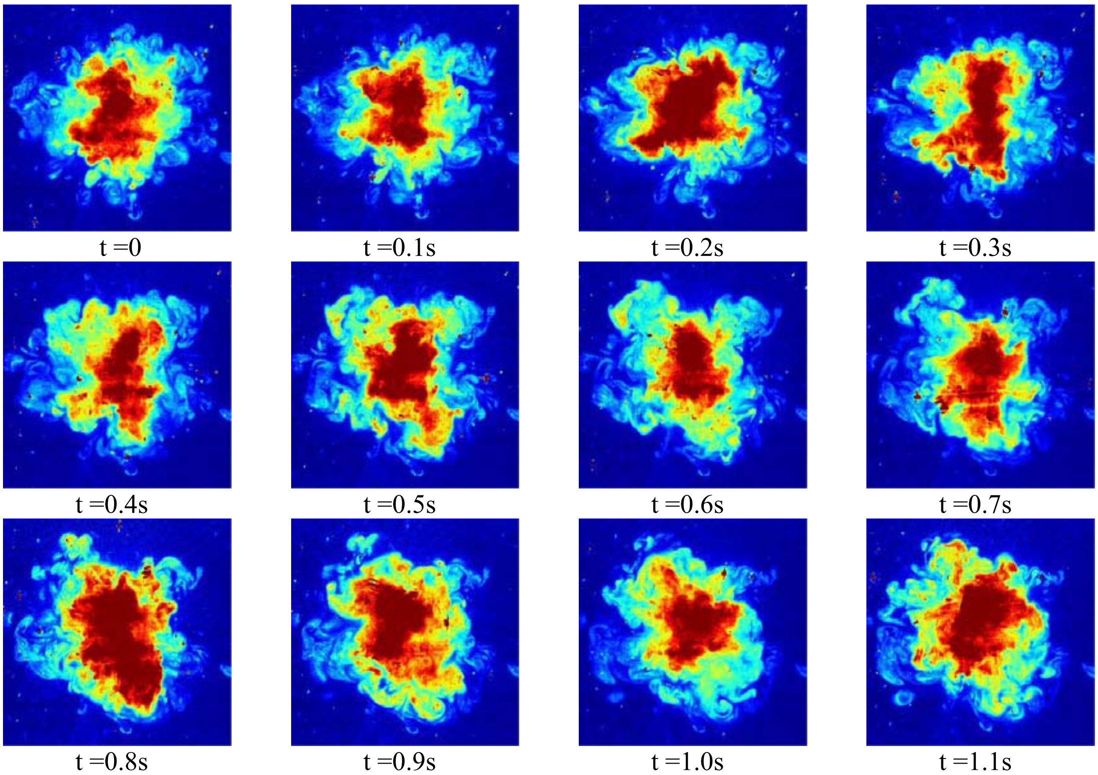

Figure C. 21: Instantaneous flow visualisation of the normalised concentration for the primary jet at *x/D*=6, at 0.1 second intervals and λ = 0 γ=0, κ =0.

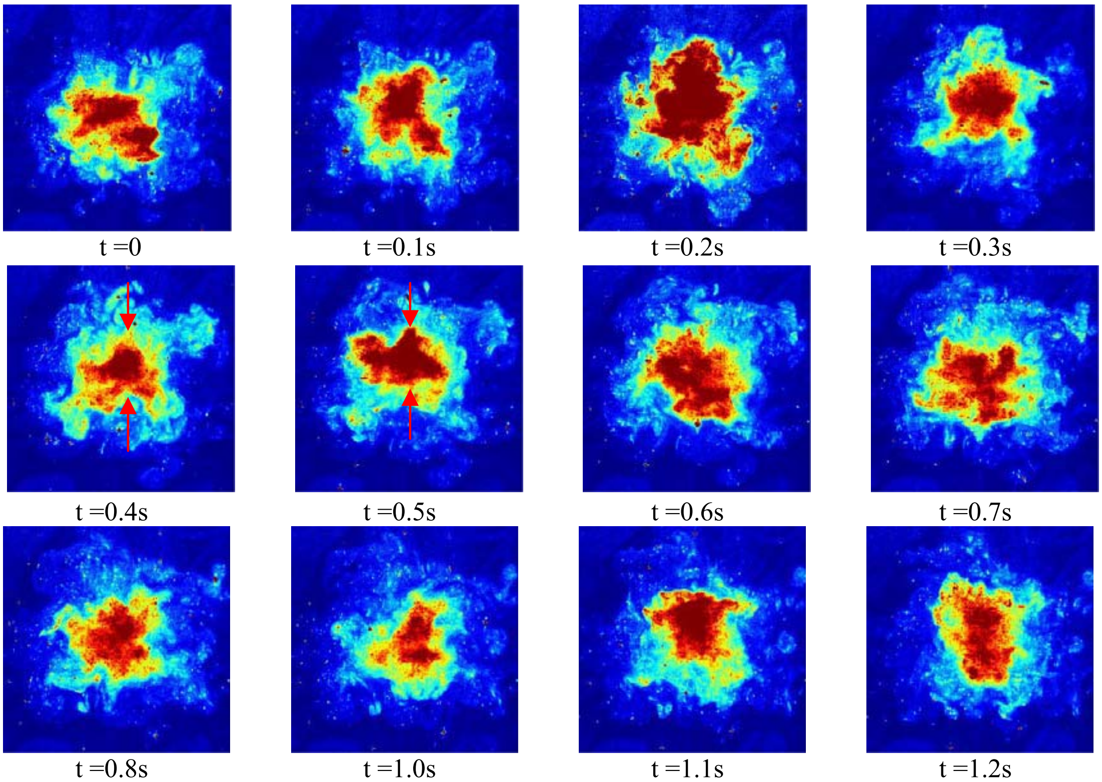

Figure C. 22: Instantaneous flow visualisation of the normalised concentration for the primary jet at *x/D*=6, at 0.1 second intervals and λ = 0.55, γ=0.3, κ =0.18. The red arrows highlight the out of phase shortening of the jet in the *y*-direction.

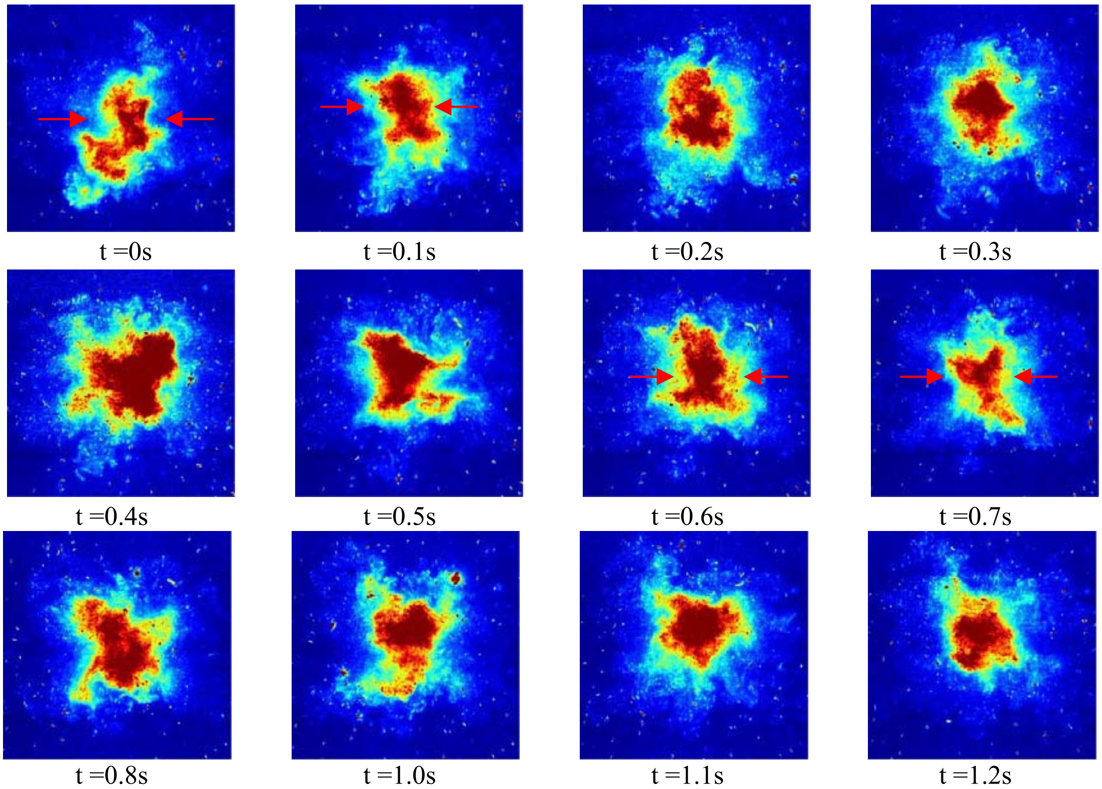

Figure C. 23: Instantaneous flow visualisation of the normalised concentration for the primary jet at *x/D*=6, at 0.1 second intervals and λ = 1.4, γ=1.96, κ =1.18. The red arrows highlight out of phase shortening of the jet in the *z*-direction.

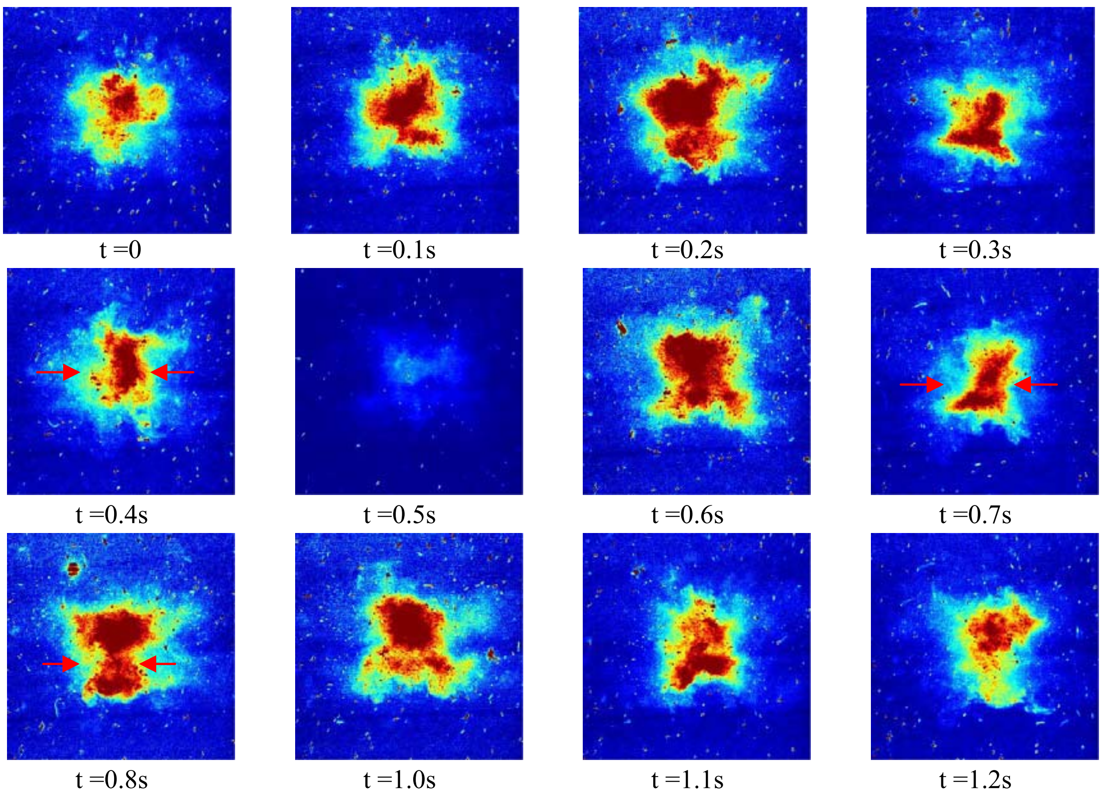

Figure C. 24: Instantaneous flow visualisation of the normalised concentration for the primary jet at *x/D*=6, at 0.1 second intervals and λ = 2.8, γ=7.84, κ =4.7. The red arrows highlight out of phase shortening of the jet in the *z*-direction.

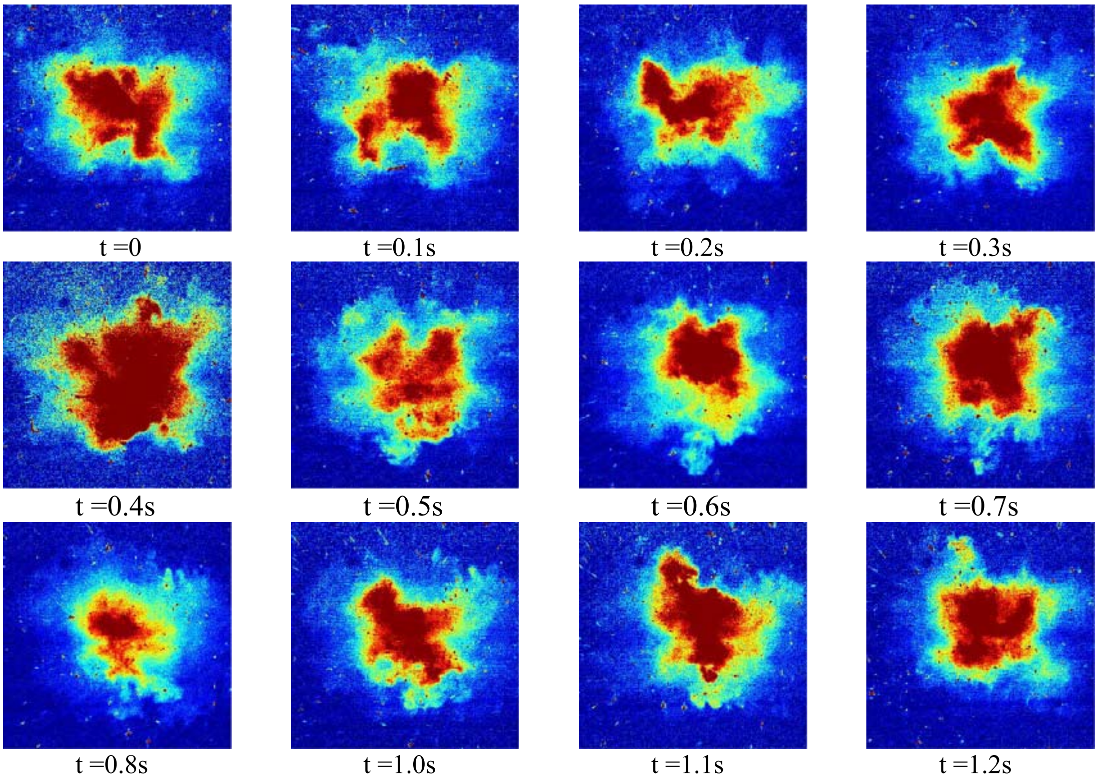

Figure C. 25: Instantaneous flow visualisation of the normalised concentration for the primary jet at x/D=6, at 0.1 second intervals and λ = 3.6, γ=12.96, κ =7.78.

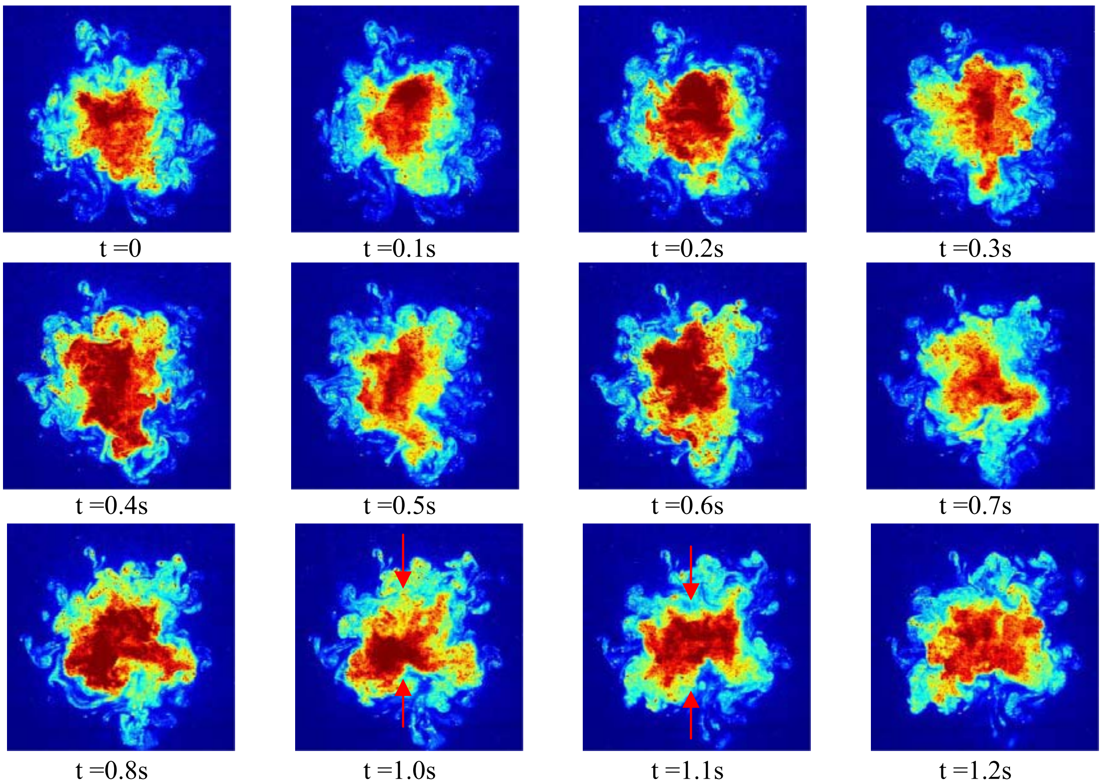

Figure C. 26: Instantaneous flow visualisation of the normalised concentration for the primary jet at x/D=8, at 0.1 second intervals and λ = 0, γ=0, κ =0.

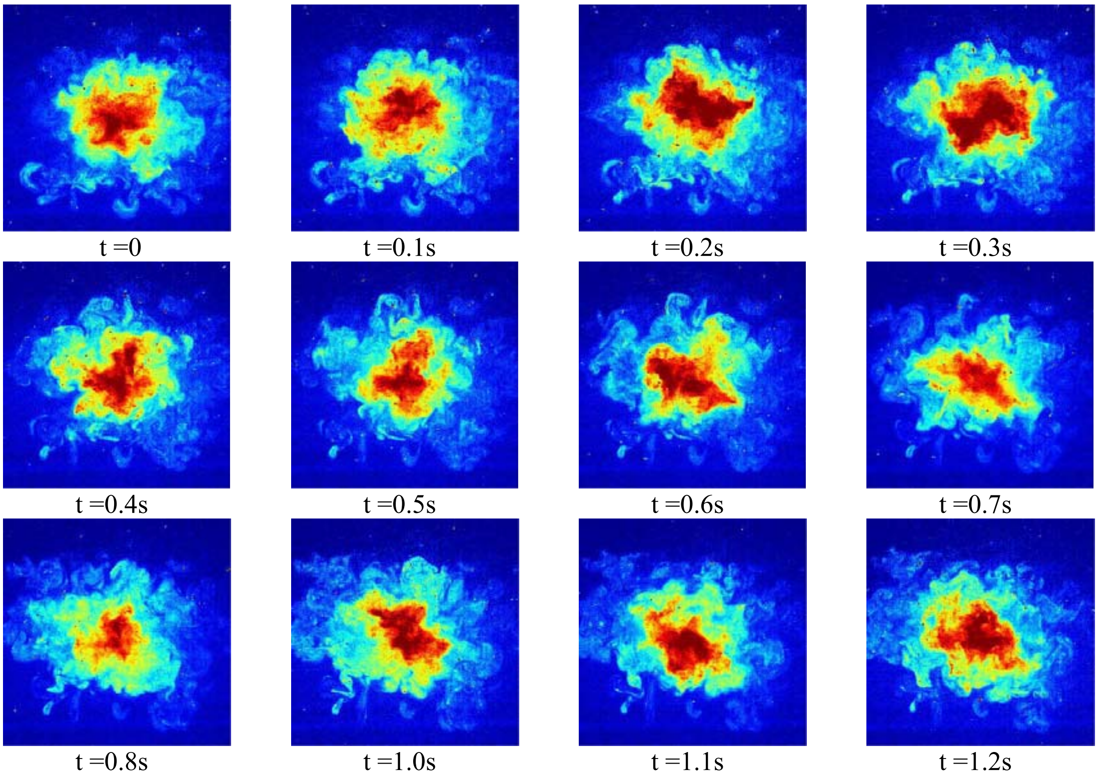

Figure C. 27: Instantaneous flow visualisation of the normalised concentration for the primary jet at x/D=8, at 0.1 second intervals and λ = 0.55, γ=0.3, κ =0.18.

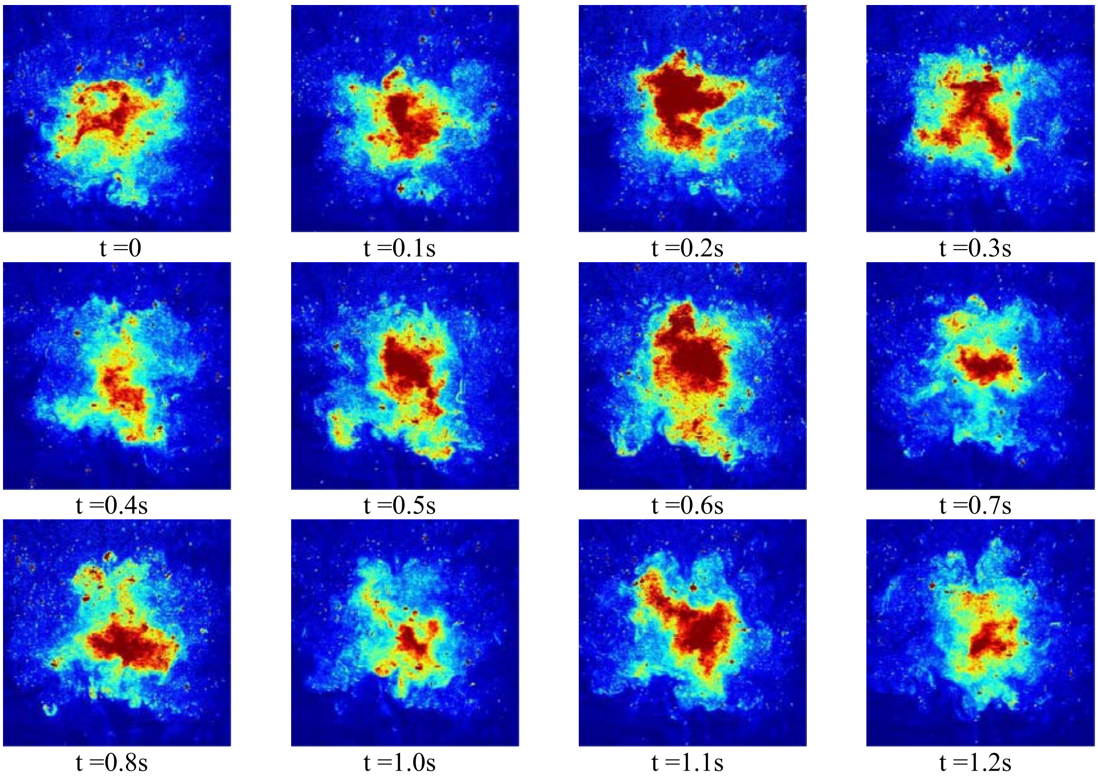

Figure C. 28: Instantaneous flow visualisation of the normalised concentration for the primary jet at x/D=8, at 0.1 second intervals and λ = 1.4, γ=1.96, κ =1.18.

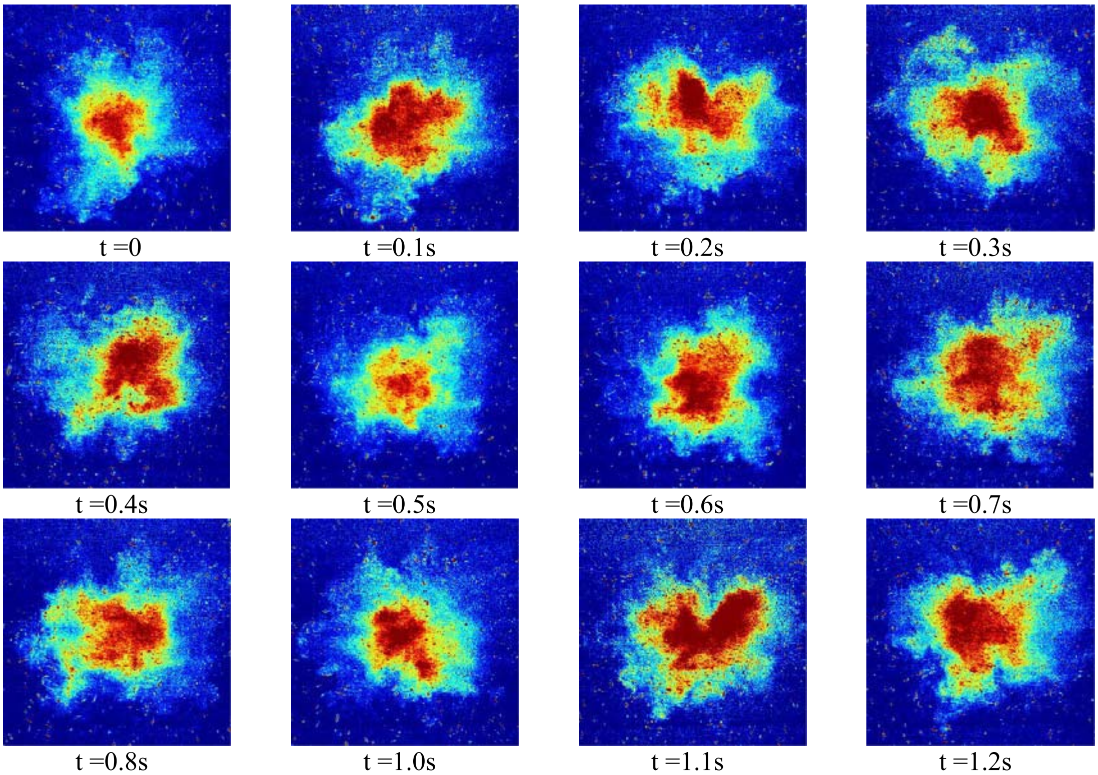

Figure C. 29: Instantaneous flow visualisation of the normalised concentration for the primary jet at x/D=8, at 0.1 second intervals and λ = 2.8 γ=7.84, κ =4.7.

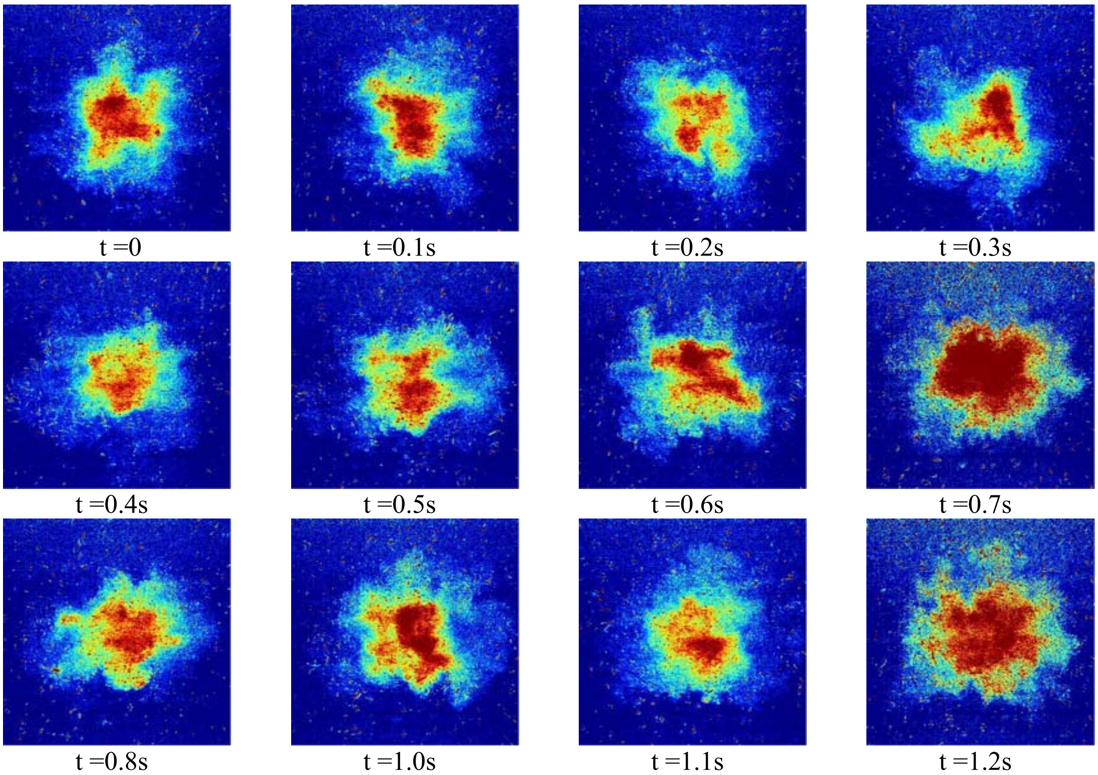

Figure C. 30: Instantaneous flow visualisation of the normalised concentration for the primary jet at x/D=8, at 0.1 second intervals and λ = 3.6, γ=12.96, κ =7.78.